Genes and Immunity (2007) 8, 262–274

www.nature.com/gene

ORIGINAL ARTICLE

Splenic and immune alterations of the Sparc-null mouse accompany a lack of immune response

SA Rempel[1], RC Hawley[2], JA Gutiérrez[2], E Mouzon[1], KR Bobbitt[3], N Lemke[1], CR Schultz[1], LR Schultz[4], W Golembieski[1], J Koblinski[5], S VanOsdol[5] and CG Miller[3]

[1]*Department of Neurosurgery, Barbara Jane Levy Laboratory of Molecular Neuro-Oncology, Hermelin Brain Tumor Center, Henry Ford Hospital, Detroit, MI, USA;* [2]*Department of Pathology, Henry Ford Hospital, Detroit, MI, USA;* [3]*Department of Neurosurgery, Gayle Halperin Kahn Laboratory of Viral Onco-Therapeutics, Hermelin Brain Tumor Center, Henry Ford Hospital, Detroit, MI, USA;* [4]*Department of Biostatistics and Research Epidemiology, Henry Ford Hospital, Detroit, MI, USA and* [5]*NIDCR, NIH, Bethesda, MD, USA*

Sparc-null mice have been used as models to assess tumor-host immune cell interactions. However, it is not known if they have a competent immune system. In this study, the immune systems of Sparc wild-type and null mice were compared. Mice were assessed for differences in total body weight, spleen weight and spleen-to-body weight ratios. Spleens were compared with respect to morphology, and Sparc, Ki-67, MOMA-1 and IgM expression. Immune cells in blood, bone marrow and spleen were assessed by blood smears, automated blood panel, and flow cytometry. Additionally, the ability of Sparc-null mice to respond to immune challenge was evaluated using a footpad model. The morphological and immunohistochemical results indicated that Sparc-null spleens had more white pulp, hyperproliferative B cells in the germinal centers, and decreased marginal zones. Sparc-null spleens lacked normal Sparc expression in red and white pulp, marginal zones, endothelial and sinusoidal cells. By flow analysis, B cells were decreased and T cells were increased in the bone marrow. Finally, Sparc-null mice were unable to mount an immune response following footpad lipopolysaccharide challenge. These data confirm that Sparc-null mice have an impaired immune system.
Genes and Immunity (2007) **8,** 262–274. doi:10.1038/sj.gene.6364388; published online 8 March 2007

Keywords: *SPARC; Sparc-null mouse; immune cells; spleen; marginal zone*

Introduction

SPARC (osteonectin, BM-40) is a secreted matricellular protein involved in the modulation of cell adhesion and motility. *Sparc*-null mice have been generated[1,2] to examine its roles in development and disease. The first major phenotype reported was the development of cataracts 6–8 months postnatally.[1,2] Since then, additional phenotypes have been described including osteopenia,[3] increased fat deposition,[4] altered wound healing[5] and altered collagen deposition.[6]

SPARC has also been implicated in tumor progression. However, seemingly disparate results have been obtained, depending on the tumor type studied.[7] For some cancers, such as ovarian cancer, the loss of *SPARC* is associated with progression[8,9] and the re-expression of *SPARC* in ovarian tumor cells induces apoptosis.[10] Similarly, aggressive neuroblastomas have little *SPARC* expression in the tumor cells, whereas *SPARC* is expressed in the surrounding stromal cells. Treatment of the tumors with *SPARC* peptides *in vivo* inhibited tumor growth.[11,12] In contrast, *SPARC* is highly expressed in melanoma[13] and gliomas.[14] The inhibition of *SPARC* expression in melanoma cells[15] and the overexpression of *SPARC* in glioma cells[16,17] promoted decreased adhesion and increased migration, respectively, suggesting that increased *SPARC* expression in these cancer types promotes invasion. That *SPARC* may be associated with good prognosis for some cancers, but worse prognosis for others, may in fact be due to the difference in expression patterns, that is, tumor cells versus stromal cells, the latter including resident immune cells. The generation of *Sparc*-null mice has provided a means to examine the role of *Sparc* in these specific compartments.

In a study by Sangaletti *et al.*,[18] *SPARC*-expressing mammary tumor cells were injected into the mammary fat pad of *Sparc*-null and wild-type (WT) mice. Tumor cells injected into WT mice developed tumors with lobular structures having well-defined septa expressing high levels of collagen IV, and infiltrating immune cells. *Sparc* was expressed in both immune and tumor cells. When tumor cells were injected into *Sparc*-null mice, where *Sparc* expression was limited to the tumor cells, the tumors displayed an increased number of infiltrating immune cells. However, the resultant tumors were less well structured, having smaller septa and less collagen IV. These data indicated that *Sparc* produced by the host

Correspondence: Dr SA Rempel, Department of Neurosurgery, Hermelin Brain Tumor Center, Henry Ford Hospital, 2799 West Grand Blvd., Detroit, MI 48202, USA.
E-mail: nssan@neuro.hfh.edu
Received 11 December 2006; revised and accepted 1 February 2007; published online 8 March 2007

leukocytes determined the assembly and function of tumor-associated stroma through the organization of collagen type IV. In contrast, several other studies indicate that a loss of host *Sparc* augments tumor progression,[9,19,20] suggesting fundamental differences in the role of *Sparc* and the regulation of growth in different tumor types. However, all of the studies reported a decreased extracellular matrix (ECM) and an increase in infiltrating macrophages with the loss of host *Sparc*. These studies however, did not address the role of *Sparc* in the leukocytes with respect to their ability to modulate an immune response.

That *Sparc* expression by tumor cells helps the cells escape from immune surveillance is supported by a study by Alvarez *et al*.[21] They demonstrated that the inhibition of *Sparc* expression in melanoma cells implanted into nude mice promoted polymorphonuclear (PMN) leukocyte recruitment to the tumor, and importantly, that the PMNs suppressed tumor growth. However, PMNs are the first line of immune defense, and the study is limited by the inability to study a fully competent immune system using a nude mouse model.

Several studies suggest possible differences in underlying immune responses between *Sparc*-null and WT mice. Increased neutrophil and leukocyte infiltration was observed in bleomycin-induced peritonitis[22] and in TPA-induced skin inflammation[18] in the knockouts. However, these studies did not address the underlying mechanism with regards to the need for *Sparc* expression by the leukocytes or in the ECM in the differences observed. In a follow-up study, Sangaletti *et al*.[23] examined Langerhan cell (LC) migration and the ability to impact T-cell priming in cutaneous contact hypersensitivity (CHS) in *Sparc* WT and null BALB/cAnNCrl mice, and in WT and null mice previously irradiated and rescued with null or WT bone marrow cells, respectively. These studies demonstrated that the loss of *Sparc* expression did not alter the inherent ability of the LCs to migrate. However, the lack of *Sparc* expression altered the ECM, thereby decreasing the physical barrier confronting the LCs and hastening migration to lymph nodes, which accelerated the onset of T-cell priming. In this case, loss of *Sparc* in the stroma rather than loss of expression by immune cells appeared to be important in controlling the extent of CHS. In contrast, *Sparc*-expressing SKH-1 mice demonstrated greater CHS response to oxazolone than SKH-1/*Sparc*-null mice.[24] Differences in outcome may be due to the use of different strains of mice and/or different sensitizing agents.

Therefore, although these studies have examined the role of *Sparc* expression in local immune reactions, either by immune cells or by tumor cells, none have addressed the global significance of *Sparc* in the development of a competent immune system.

We have also been breeding *Sparc*-null and WT mice. At two institutions, we observed that several of the aged *Sparc*-null mice that were injured developed infections that did not heal, requiring the mice to be killed. These observations suggested differences in the ability of the immune systems to respond to infection, suggesting that *Sparc*-null mice were immune compromised. This could potentially impact the interpretation of tumor-immune cell interactions. This prompted us to analyze the immune system in *Sparc* WT and null mice that had not been in any way treated or subjected to tumor implant. We examined the mice for differences in total body weight, and the weights, morphology, and *Sparc*, Ki-67, MOMA-1 and IgM expression in the spleens. Furthermore, differences in immune cell populations were assessed by blood smears, automated blood panel, and flow cytometry of bone marrow, blood and spleen compartments. Finally, response to immune challenge was assessed.

Results

Generation of Sparc *WT and null mice*

Polymerase chain reaction (PCR) genotyping for the *Sparc*-null and WT alleles demonstrated the generation of both populations (Figure 1a). The loss of *Sparc* expression in null spleens is represented by Western blot analysis using anti-*Sparc* antibody (Figure 1b).

Sparc-*nulls have larger spleens and a greater spleen/body weight ratio*

We saw no statistically significant difference in the overall body weight between *Sparc* WT and null mice when assessed by genotype (Figure 1c), or by gender within a genotype (Figure 1d). No differences in wet or dry weights were observed for any organs from WT and null mice, including another immune organ, the thymus (Figure 1e and f), except for the spleens (Figure 1g and h). Gross changes in size are illustrated in the Figure 1g inset. The null mice had higher spleen wet weights (approximately 1.5-fold (Figure 1g)), consistent for both genders (Figure 1h). A similar trend was observed for dry weight. In addition, the larger spleens represented a greater percentage of the total body weight (Figure 1i), also consistent for both genders (Figure 1j).

Localization of Sparc *expression in WT spleens*

Assessment of *Sparc* expression by Western blot analysis suggested that the protein might be expressed in the spleens. Alternatively, it could be a signal derived from trapped circulating cells, such as platelets. Immunohistochemical analysis indicated that *Sparc* is normally expressed sparsely in endothelial cells within the

Figure 1 *Sparc*-null (Null) mice have a larger spleen and a greater spleen-to-body weight ratio compared with *Sparc* WT (WT) mice. (**a**) PCR genotyping of null and WT mice using *Sparc*-specific primers as described in Materials and methods. ^ – The lanes are on the same gel, but moved closer. (**b**) Western blot analysis demonstrating the lack of *Sparc* protein in the spleen from null versus WT mice. ^ – The ladder is on the same gel, but moved closer. Actin was used as a loading control. (**c** and **d**) A comparison of total body weight indicates no differences between null and WT genotypes (**c**) or between genders/genotype (**d**). (**e** and **f**) A comparison of wet and dry weights for thymus organs indicates no differences between null and WT genotypes (**e**) or between genders/genotype (**f**). A comparison of spleen wet and dry weights indicates that the spleens are larger in null compared with WT mice (**g**, inset illustrating the spleens immediately after removal). Differences in wet and dry weights are maintained for both genders within a genotype (**h**). The ratio of spleen weight to 100 g total body weight is greater for null mice than for WT mice (**i**). This difference in ratio is maintained between genders (**j**), $n = 17$ null and $n = 11$ WT; of these, $n = 14$ male subjects, $n = 14$ female subjects.

lymphoid follicles and marginal ones, and more profusely in sinusoids and cells of the red pulp (Figure 2e–h). Loss of *Sparc* expression was confirmed in the null spleens (Figure 2a–d).

Sparc-*null spleens differ in morphology*

As cells within the spleen normally express *Sparc*, we compared WT and null spleens to determine whether morphological changes accompanied the loss of its

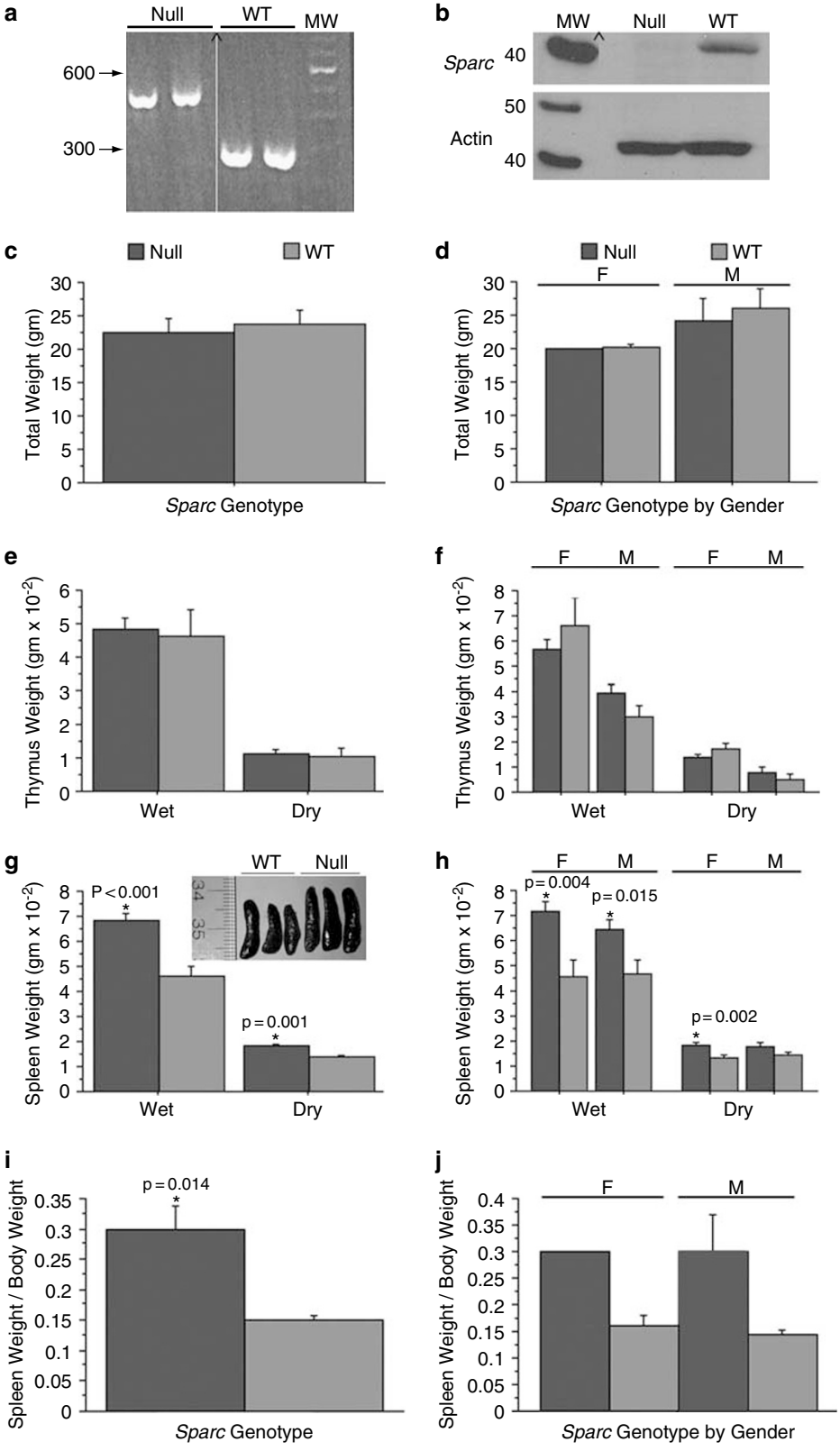

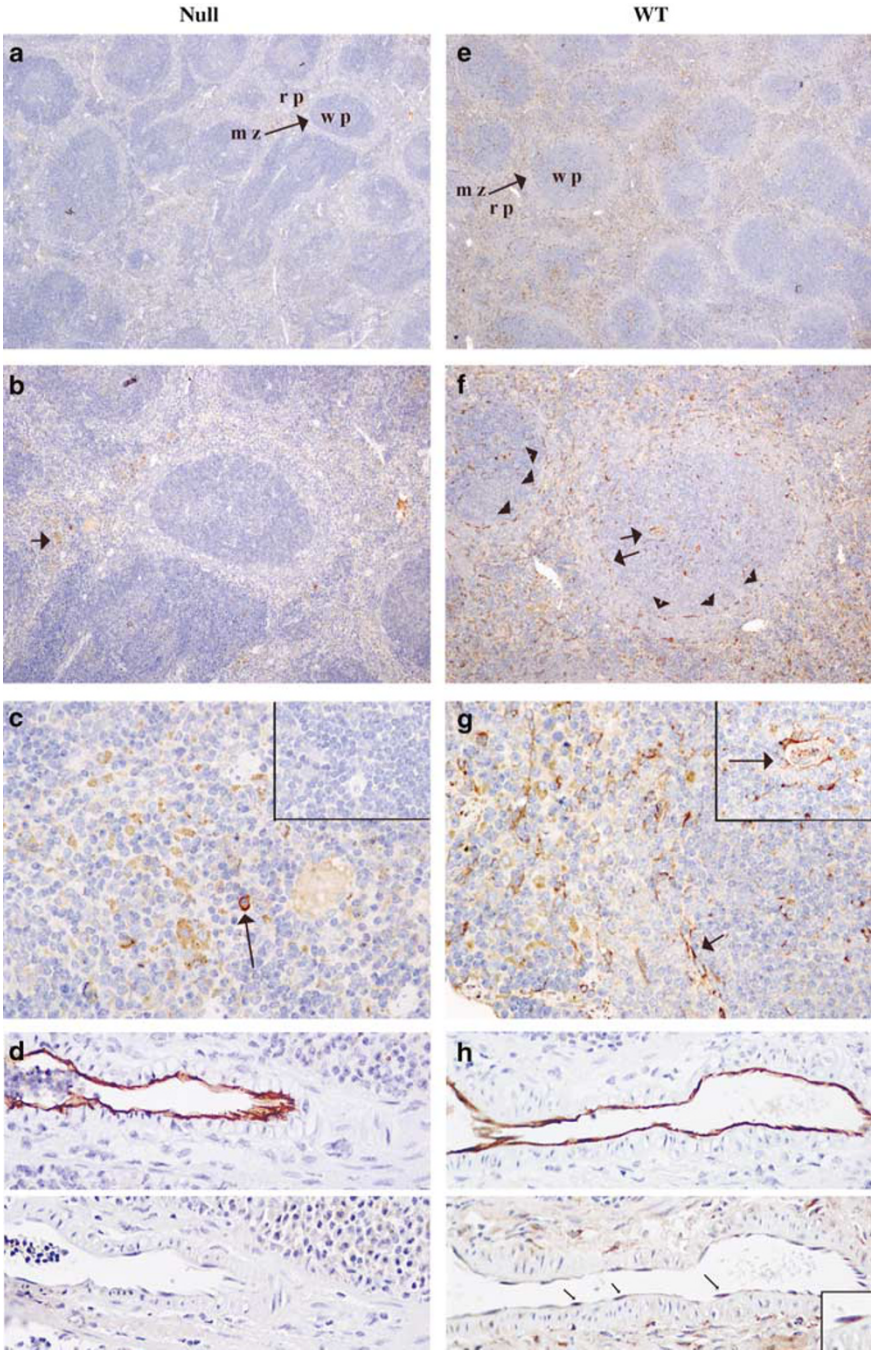

Figure 2 *Sparc* localization in WT spleens and confirmation of loss in *Sparc*-null spleens. (**a–h**) Representative formalin-fixed, paraffin-embedded spleen sections from *Sparc*-null (**a–d**) and *Sparc* WT (**e–h**) mice were immunohistochemically stained for *Sparc* or CD31 (**d**, **h**; top panels) expression. Magnifications are $\times 40$ (**a, e**), $\times 100$ (**b, f**) and $\times 400$ (**c**, **d**, **g**, **h**). The regions of red pulp (rp), white pulp (wp) and marginal zones (mz, arrows) indicated in **a** and **e**, are magnified in (**b–c**) and (**f–g**), respectively. *Sparc* expression is observed in endothelial cells within the white pulp (**f**, **g**; inset) and in the sinusoidal cells (**f**, arrowheads; **g**, arrow indicating magnified region in **f**). A punctate staining pattern is observed throughout the red pulp (**g**) and white pulp (**g** inset). *Sparc* expression is absent in the *Sparc*-null spleens as expected (**a–d**). Rarely, an immunoreactive cell is observed suggesting minimal non-specific cross-reactivity (**c**, arrow; WP: inset). A background signal is observed in both *Sparc*-positive and *Sparc*-negative spleens due to hemosiderin granules. Endothelial cells were identified using CD31 antibody (**d**, **h**: top panels). Endothelial cells in WT spleens (arrows) are *Sparc*-positive (**h**; lower panel; inset: magnification of an endothelial cell). Endothelial cells of *Sparc*-null spleens are negative (**d**: lower panel) ($n = 4$/genotype).

expression. In the *Sparc*-null spleens, there was expansion of B-cell-rich nodular white pulp and an increased number of secondary lymphoid follicles (Figure 3a–c) in comparison to the WT spleens (Figure 3d–f). The follicular lymphoid hyperplasia in the null spleens was characterized by prominent germinal centers with numerous centroblasts, centrocytes, mitotic figures, and readily apparent tingible-body macrophages. In addi-

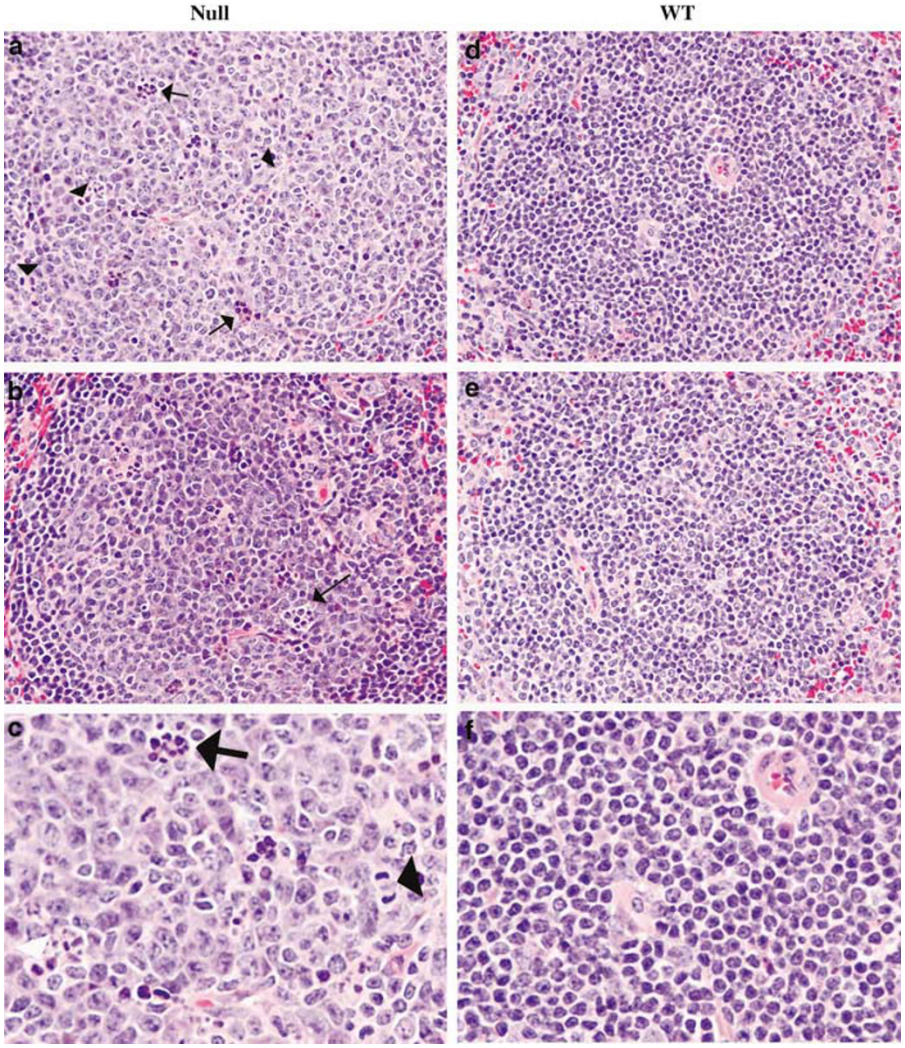

Figure 3 Spleens from *Sparc*-null mice are morphologically different. (**a–f**) H&E-stained, formalin-fixed, paraffin-embedded and sectioned spleens from *Sparc*-null (**a**, **b**, **c**) and *Sparc* WT (**d**, **e**, **f**) mice. In the null spleens, the secondary (hyperplastic) follicles are better circumscribed than those in the WT spleens, with germinal centers containing numerous centroblasts (large nuclei, prominent nucleoli, and appreciable, pink cytoplasm) and centrocytes. There are frequent tingible-body macrophages (arrows) and mitotic figures (arrowheads). For the WT spleens, the primary lymphoid follicles are rather ill-defined and sparsely cellular, with prominent marginal zones. Both tingible-body macrophages and mitotic figures are inconspicuous. There were no gender differences within a genotype for male subject (**a**, **c** and **d**, **f**) or female subject (**b**, **e**) spleens. Images are at $\times 600$ magnification (**a**, **b**, **d**, **e**). Regions in **a** and **d** were further magnified ($\times 1200$) in (**c**, **f**) respectively, using Photoshop software), $n = 8$/genotype.

tion, the marginal zones appeared distinctly attenuated in the null spleens. The T-cell-rich periarteriolar lymphatic sheaths (although perhaps slightly hypercellular) were unremarkable. No differences in morphology were observed for any other organs.

Sparc-*null spleens have greater numbers of proliferative follicular B cells*

The follicular hyperplasia observed by morphology was confirmed and quantitated using the proliferation marker Ki-67. The *Sparc*-null spleens demonstrated significantly greater numbers (approximately 3.6-fold) of proliferating germinal center cells (Figure 4a) in comparison with the WT (Figure 4c). On average, the WT spleens had an average of 166.5 ± 34 SE Ki-67$^+$ cells/follicle in comparison with the null spleens that had an average of 602.7 ± 22 SE Ki-67$^+$ cells/follicle ($P < 0.0001$; Figure 4e). Analysis of Ki-67 staining within the red pulp indicated no statistical differences between WT and null spleens (data not shown).

Sparc-*null spleens have more white pulp per given area*

To determine whether the loss of *Sparc* altered the overall amount of white pulp, the percentage of splenic tissue comprised of white pulp was measured. On average, the *Sparc*-null spleens had more white pulp than normal spleens ($P = 0.0245$; Figure 4f).

Sparc-*null spleens have smaller marginal zones*

The splenic marginal zones were assessed by counting the cell layers within this compartment. The bars indicate marginal zones in Ki-67-stained (Figure 4a and c) and adjacent hematoxylin and eosin (H&E)-stained (Figure 4b and d) sections. WT spleens had larger marginal zones

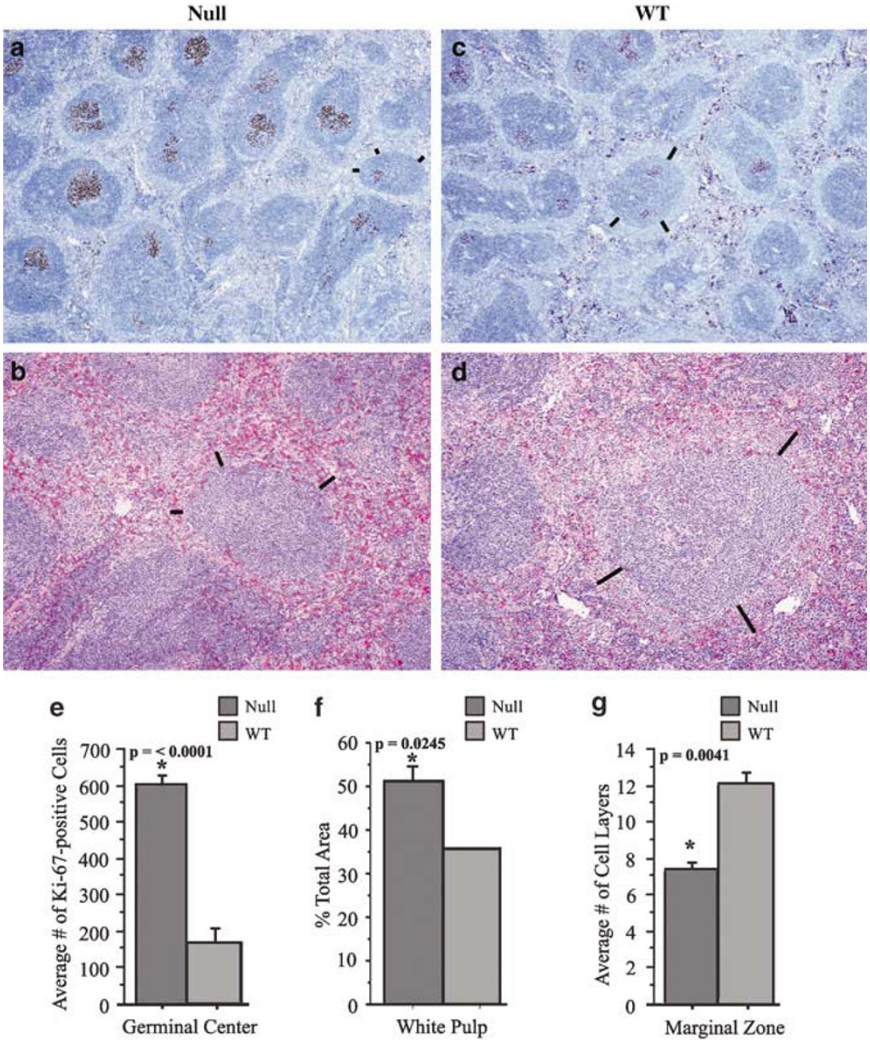

Figure 4 *Sparc*-null mice have spleens with greater numbers of proliferating germinal center B cells, more white pulp and smaller marginal zones. (**a** and **c**) Ki-67 expression in formalin-fixed, paraffin-embedded and sectioned spleens from *Sparc*-null (**a**) and *Sparc* WT (**c**) mice. Greater numbers of proliferative B cells were observed within the germinal centers of *Sparc*-null spleens. Images are at $\times 40$ magnification, $n=4$/genotype. (**b** and **d**) H&E-stained formalin-fixed, paraffin-embedded sections of spleens from *Sparc*-null (**b**) and *Sparc* WT (**d**) mice. Images are at $\times 100$ magnification of regions identified by bars in (**a** and **c**). Bars indicate marginal zones, which are attenuated in the *Sparc*-null spleens, $n=4$/genotype. (**e**) The number of Ki-67-positive germinal center B cells/follicle was counted and averaged/spleen. The averages/genotype were then plotted, $n=4$/genotype. (**f**) The percent area of white pulp/spleen was measured. The averages/genotype were plotted, $n=4$/genotype. (**g**) The number of cell layers/marginal zone/follicle was counted and averaged/spleen, $n=4$/genotype.

(Figure 4d) with an average of 12.2 cell layers (Figure 4g) in contrast to the *Sparc*-null marginal zones (Figure 4b), which had an average of 7.4 cell layers (Figure 4g). These results are significantly different ($P=0.0041$).

Immunohistochemical assessment of marginal zones development

To further evaluate marginal zone formation, spleens were immunohistochemically stained with MOMA-1 and anti-IgM antibodies. MOMA-1 antibody was used to delineate marginal metallophilic macrophages (MMM) that line the inner border of the sinus margin and, in effect, demarcate the boundary between white pulp and marginal zone. Anti-IgM antibody was employed to identify marginal zone B cells, which tend to express high levels of IgM. In tandem, these immunostains demonstrated a normal complement of MMM in both WT and null spleens, and confirmed the decrement in IgM+ marginal zone B cells just outside the MMM in the *Sparc*-null spleens (Figure 5).

Quantitation of white blood cells in blood smears

Blood smear analysis permits not only a count of the numbers of cells, but also allows an assessment of blood cell morphology. There were no significant differences in the blood cell morphology between *Sparc*-null and WT mice. In addition, there were no significant differences in total counts for monocytes, granulocytes or lymphocytes as assessed by genotype (Figure 6a) or when split by gender (Figure 6b). Although the slightly higher number of lymphocytes in the *Sparc*-null mice was not significant, it did suggest the possibility of an increase in a sub-population of lymphocytes.

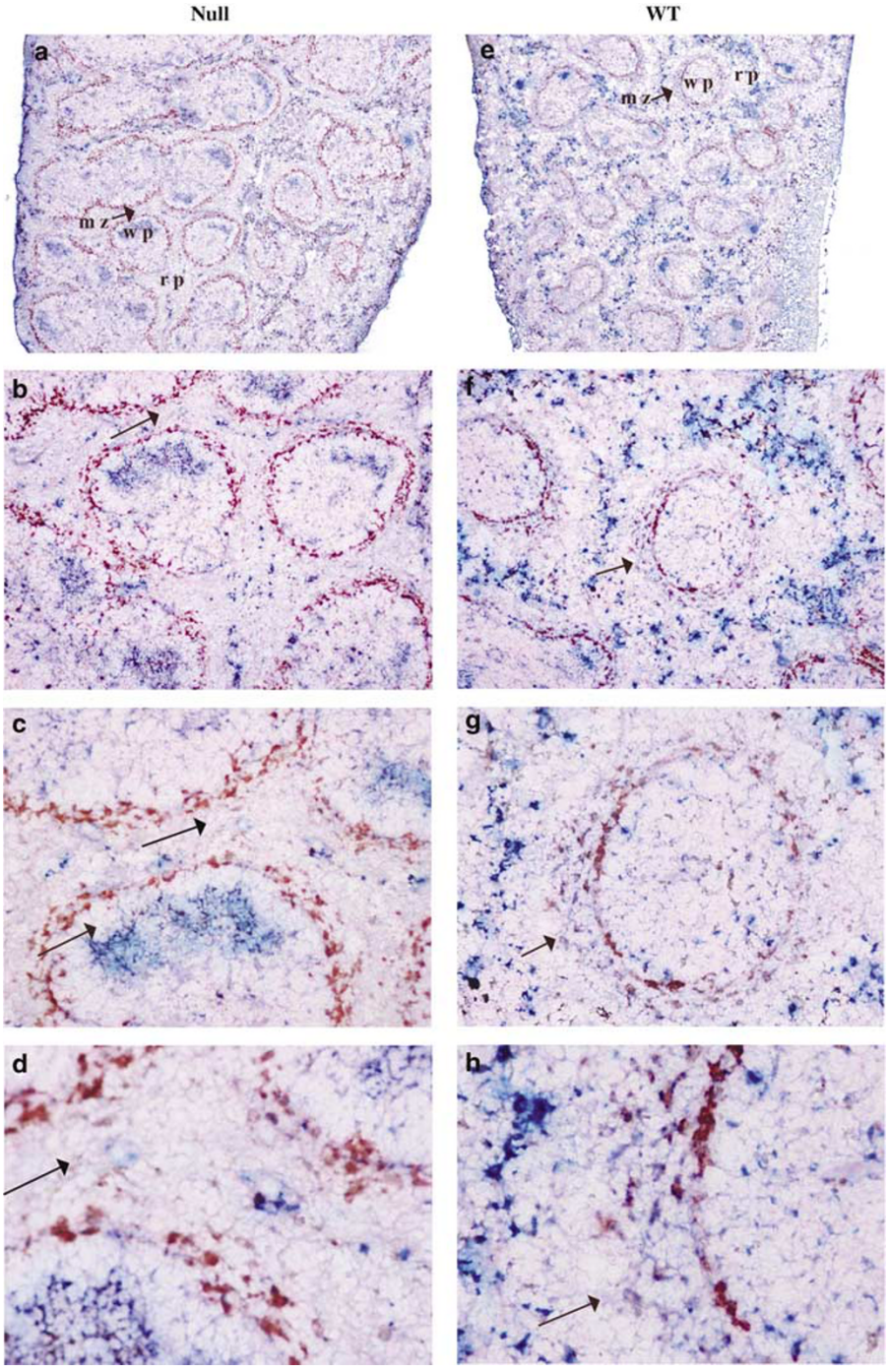

Figure 5 *Sparc*-null spleens have enlarged white pulp and fewer IgM-expressing marginal zone B cells. (**a**–**h**) Representative *Sparc*-null (**a**–**d**) and WT (**e**–**h**) spleens were immunohistochemically stained with MOMA-1 antibody to detect MMM (red) and with anti-IgM to detect marginal zone B cells (blue). Note: IgM expression is not restricted to marginal zone B cells. Magnifications are $\times 40$ (**a**, **e**), $\times 100$ (**b**, **f**), $\times 200$ (**c**, **d**) and $\times 400$ (**d**, **h**). (**b**–**d** and **f**–**h**) Images are increasing magnifications of the red pulp (rp), white pulp (wp) and marginal zones (mz, arrrows) indicated in (**a** and **e**), respectively. Note the increased size of follicles (**a** versus **e**) and the decrease in IgM-positive marginal zone B cells (**a**–**d** versus **e**–**h**) in the *Sparc*-null versus WT spleens, respectively, $n = 3$/genotype.

Hematologic analyses

An automated blood panel was performed to define the cellular components more clearly (Table 1). In agreement with the blood smears, no differences were observed for monocytes, and neutrophils were significantly lower in the *Sparc*-null mice. In addition, no differences were observed between eosinophils and basophils. In agreement with the trends observed by the blood smears, this analysis demonstrated a slight but significant increase in lymphocytes of the *Sparc*-null mice, even though the total white blood cells (WBCs) were significantly lower (Table 1). Owing to the gross morphological differences in the spleen, subsequent analyses focused on the lymphocyte compartment.

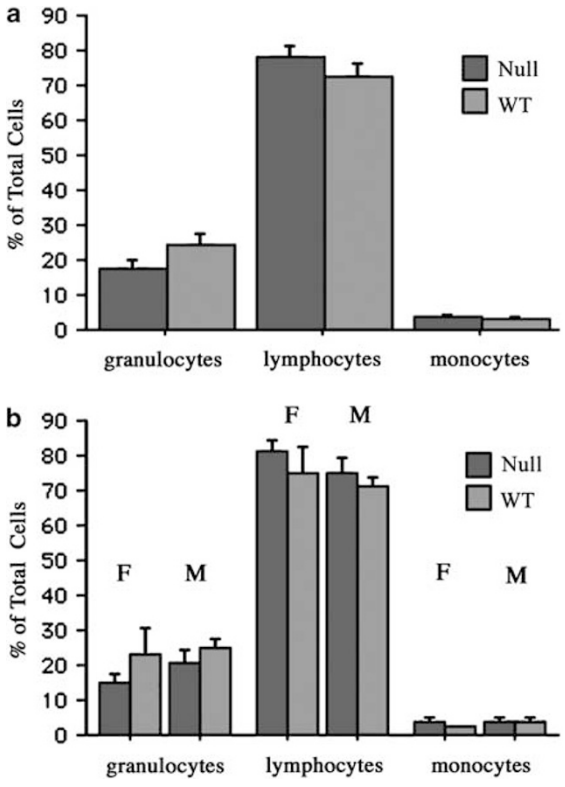

Figure 6 Blood smears demonstrate a trend towards an increased lymphocyte population in *Sparc*-null mice. (**a**) Blood smears were counted and the percentage of granulocytes, lymphocytes and monocytes are illustrated for *Sparc*-null (Null) versus *Sparc* WT (WT) mice. (**b**) The cell percentages were plotted by gender. Although no statistically significant differences are observed, the data suggest a trend for decreased granulocytes and increased lymphocytes in the *Sparc*-null blood smears, $n=17$ null, $n=11$ WT.

Table 1 Hematologic assessment

Genotype	Sparc-*null*		Sparc *WT*		P-*value*
Blood analysis	n	*Mean*±*s.e.*	n	*Mean*±*s.e.*	
White blood cells (1000/μl)	26	2.0±0.4	30	3.2±0.4	**0.0039**
% Lymphocytes	26	86.8±1.0	30	79.7±4.0	**0.0034**
% Neutrophils	26	9.4±0.5	30	15.7±3.4	**0.0038**
% Monocytes	26	2.9±0.3	30	3.8±0.6	0.1611

Abbreviations: *n*, number of mice; s.e., standard error; WT, wild type.
Automated hematologic assessment averaged over three separate experiments using the ABX Pentra 60C+ system. Standard errors take into account data from three separate experiments. *P*-values from Generalized Estimating Equations models are provided.
Statistically significant *P*-values are in bold.

Flow cytometric immunoanalysis of Sparc-*null and WT lymphocytes isolated from bone marrow, blood and spleens*

We performed flow cytometric immunoanalysis on bone marrow, blood and spleens to determine if there were differences in major lymphocyte subsets in the *Sparc*-null versus WT mice. Statistically significant differences were observed only for bone marrow lymphocytes, which revealed a relative increase in CD3+ cells (T cells) and a relative decrease in CD19+ cells (B cells) in the *Sparc*-null mice (Table 2). A representative flow cytometric analysis is illustrated for CD3 and CD19 markers (Figure 7).

Table 2 Bone marrow, blood and spleen lymphocyte subset marker analyses

Genotype	Sparc *WT*		Sparc-*null*		P-*value*
Source	n	*Mean*±*s.d.*	n	*Mean*±*s.d.*	
BM lymphocytes					
CD19	4	54.5±4.9	4	44.9±3.8	**0.022**
CD3	5	27.3±2.7	4	35.8±5.5	**0.019**
Blood					
CD19	9	28.8±12.2	9	31.9±9.5	0.553
CD3	9	49.3±11.0	7	45.2±9.6	0.441
Spleen					
CD19	10	57.4±13.1	8	59.8±13.7	0.704
CD3	9	29.3±2.6	8	33.6±6.4	0.115

Abbreviations: BM, bone marrow; *n*, number of mice; s.d., standard deviation; WT, wild type.
The bone marrow lymphocyte values are gated subpopulations of the entire bone marrow cell population. *P*-values from two sample *t*-tests are provided.
Statistically significant *P*-values are in bold.

Ability to activate an immune response

As the data suggested alterations in immune cell numbers in the different compartments, the ability of the immune system of *Sparc*-null mice to activate a response was evaluated by the footpad swelling response. As can be seen in Figure 8, WT mice had a normal swelling response to the injection of lipopolysaccharide (LPS) over that of phosphate-buffered saline (PBS), with significant differences observed at 72 and 96 h. However, no response was observed to either LPS or PBS by the *Sparc*-null mice in comparison with the WT mice, indicating the inability to mount an immune response.

Discussion

Sparc-null and WT mice have been used to assess differences in tumor development in the absence or presence of *Sparc*. The influence of the host immune cells on ECM production is reported to play a potential role in modulating the access of the tumor to adjacent tissue. However, increased access by immune cells does not necessarily mean that the immune cells are competent and capable of mounting a proper response. In this report, we demonstrate that *Sparc*-null mice have an altered immune system and demonstrate a lack of immune response to challenge. Major differences were observed in spleen morphology and in splenic immune cell populations.

With respect to the spleen, gross observation indicated that the spleens were larger in the *Sparc*-null mice. This was not due to a difference in the overall size of the mice, as the total body weights of *Sparc*-null and WT animals were similar, in agreement with published data.[4]

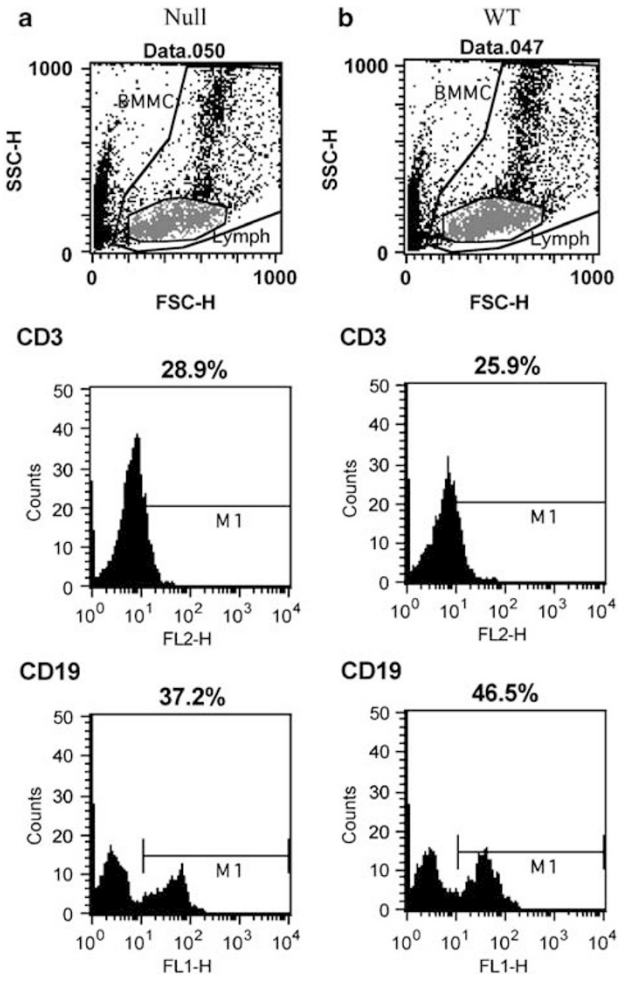

Figure 7 Characterization of *Sparc*-null lymphocyte sub-populations in bone marrow relative to sub-populations found in *Sparc* WT bone marrow. (**a**, **b**) Representative FACS analysis of total bone marrow mononuclear cell (BMMC) populations from (**a**) *Sparc*-null and *Sparc* WT mice (**b**). The total BMMC population was gated on the lymphocyte population, and the total CD3+ and CD19+ populations were determined. Lymphocytes isolated from *Sparc*-null mice have increased CD3+ populations and decreased CD19+ populations relative to the *Sparc* WT mice. Note: M1 region is based on negative control staining with fluorochrome-labeled secondary antibodies in the absence of primary antibodies, $n=10$/genotype.

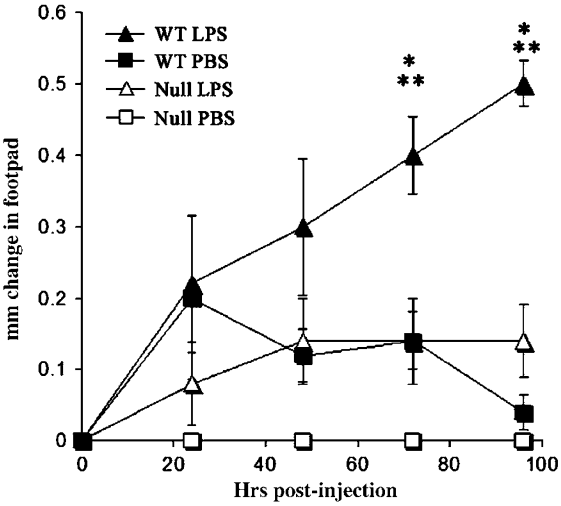

Figure 8 *Sparc*-null mice have a greatly attenuated response to LPS. LPS was injected into the footpad of *Sparc*-null (Null) and *Sparc* WT (WT) mice. Measurements were taken at time points of 0, 24, 48, 72 and 96 h and the change in footpad swelling from the 0 time point is presented. *Significant differences between *Sparc* WT LPS versus PBS treatment. **Significant differences between *Sparc* WT versus *Sparc*-null response to LPS treatment, $n=5$/genotype/treatment group.

Furthermore, the spleen to body weight ratios were significantly higher in the *Sparc*-null mice, suggesting a specific difference in the spleens. The increase in size was also not due to an increase in edema, as the wet weight and dry weight ratios remained the same.

These data suggested that *Sparc* might play a role in the spleen. We found that *Sparc* is expressed in the spleen in endothelial cells within the white pulp, in the sinusoids of the perifollicular compartment, and in scattered cells throughout the white and red pulp and marginal zones. Although our data disagree with a previous report that found no *Sparc* expression within the spleen,[25] the difference in results could be due to different fixations, antibodies and/or staining procedures. Our immunohistochemistry results are in agreement with our Western blot analysis, which also demonstrated *Sparc* in WT spleens. Furthermore, a study by Shen *et al*.[26] also found *Sparc* expression in the stromal compartment of the spleen of normal mice. Thus, we propose that the loss of *Sparc* could alter overall spleen development and growth, and/or affect lymphocyte trafficking through the spleen. Recent reports indicate that *SPARC* is a ligand for Stabilin-1,[27] a receptor present on macrophages and the noncontinuous sinusoidal cells in the spleen,[28] and a ligand for VCAM-1 that mediates leukocyte transmigration.[29] These studies support our contentions that the loss of *Sparc* could impact splenic development or alter immune responses.

Indeed, the morphological and immunohistochemical assessments resulted in two major observations. The first is that the loss of *Sparc* expression correlates with increased splenic white pulp and follicular lymphoid hyperplasia. These changes are consistent with a heightened humoral immune response, possibly due to response to a foreign or self-antigen. In addition, the fold increase in proliferation, as determined by Ki-67 detection, was sufficient to account for the fold increase by weight.

The second major observation is that there is a decrease of marginal zone cell layers and IgM-positive marginal zone B cells in the spleens of *Sparc*-null mice. In normal mice, immature, bone marrow-derived B cells in the arterial circulation can enter the spleen and flow through the splenic arterioles into the marginal sinuses. Homing chemokines can draw the B cells into the follicles where some differentiate into follicular B cells and others into marginal zone B cells. The follicular B cells can recirculate or remain in the splenic follicles ready to effect a T-cell-dependent humoral immune response to circulating antigens. Marginal zone B cells traffic to and localize in the marginal zone. Marginal zone stromal cell–B cell and B cell integrin–ECM interactions are believed to play a role in marginal zone

B-cell localization;[30,31] however, the exact mechanisms that govern this process are not entirely known. Once in the marginal zone, marginal zone B cells are strategically positioned to mount a thymus-independent type 2 antigen response to circulating antigens such as bacterial capsular polysaccharide, and to transport circulating immune complexes into the splenic follicles and activate a T-cell-dependent follicular immune response. To address the role of *Sparc* in B-cell differentiation and trafficking, MOMA-1 staining of the MMM was used to identify the follicle/marginal zone boundary.[30] The MOMA-1 staining pattern appeared normal for both WT and null spleens, suggesting that the loss of *Sparc* had no impact on the localization of these cells. However, the reduction of IgM-positive marginal zone B cells, along with the hyperplasia of white pulp in the *Sparc*-null mice, suggests several possible consequences requiring further investigation. The lack of *Sparc* may alter normal B-cell differentiation, prevent proper tracking of the marginal zone B cells into the marginal zone, contribute to poor retention of marginal zone B cells within the marginal zone, and/or promote activation of follicular and marginal zone B cells, and extramarginal zone migration of the latter.

Abnormal splenic architecture has been observed with other knockout mice. For instance, the spleens of Aiolos-null mice also have follicular hyperplasia and absent marginal zones,[32] and those of Pyk-2-deficient mice lack marginal zones.[33] In these examples, the underlying defects are thought to be intrinsic to the B cell. However, as the B cells do not appear to express *Sparc* at latter stages of development, we propose that it is the loss of *Sparc* in the sinusoidal and/or stromal cells that reduces marginal zone formation in *Sparc*-null mice. Given that *Sparc* influences ECM production and integrin-ECM interactions,[34] and is a ligand for receptors present on splenic macrophages and sinusoidal cells,[28] its loss could impact B-cell localization and retention in the marginal zone.

The *Sparc*-null mice appear to have slightly lower WBC counts and neutrophil counts in peripheral blood and a decreased proportion of CD19+ B cells together with an increased proportion of CD3+ T cells in bone marrow than their WT counterparts. However, consistent imbalances in blood and bone marrow WBC or lymphoid subsets were not identified in the *Sparc*-null mice. Nevertheless, a primary defect in lymphocyte production cannot be completely ruled out in these mice. Interestingly, it has been reported that *Sparc* is a stromal cell product that interacts with precursor B cells,[35] and it is conceivable that the loss of *Sparc* in the bone marrow compartment could adversely influence early B-cell development. Recent reports do, in fact, support a role for *Sparc* as a differentiation factor where it is implicated in early myocardial cell differentiation[36] and adrenal development.[37]

Having observed alterations in the T and B cells in the bone marrow population, and hyperplasia and altered marginal zone B cells in the spleens, we used the footpad model that could be used to assess both the innate and adaptive immune response. We found the *Sparc*-null mice could not even mount an innate response. It is of interest that in normal mice, circulating polysaccharide antigen can induce an early T-cell-independent humoral immune response mediated by splenic marginal zone B cells.[30,31] However, in this model the LPS is not circulating. Thus, the lack of immune response at this early stage suggests other immune impairments, in addition to the observed alterations.

In conclusion, these data suggest that *Sparc* may play an integral role in normal development and function of the murine immune system, and that the function of *Sparc* in this regard should be investigated further. Importantly, the data also indicate that *Sparc*-null mice with a C57BL/6 genetic background may not provide a suitable model for the assessment of the immune response to tumor, given that these mice have altered immune systems.

Materials and methods

Mice and genotyping

Sparc-null mice on a mixed 129SV/C57BL/6 background were originally obtained from Dr Chin Howe at the Wistar Institute, Philadelphia, PA, USA. The nulls were backcrossed with B6129SF1/J (Jackson ImmunoResearch Laboratories Inc., West Grove, PA, USA), which retained the C57BL/6 background. Heterozygotes were obtained to derive the *Sparc* WT (WT) controls and *Sparc*-nulls (null). Mice from 2 to 11 months of age were used: 2- to 3-month-old mice were used for morphology, weights, blood smear, automated blood analysis, flow and footpad challenge, 6-month-old mice were also used for flow, and 10- to 11-month-old mice were used for morphology, Ki-67, marginal zone, MOMA-1 and IgM analyses. Mice were age matched within all experiments.

Genotyping was assessed using PCR with 0.2 μM primers including the *Sparc* forward (5′–3′) GAT GAG GGT GGT CTG GCC CAG CCC TAG ATG CCC CTC AC; *Sparc* reverse (5′–3′) CAC CCA CAC AGC TGG GGG TGA TCC AGA TAA GCC AAG; and neomycin reverse (5′–3′) GTT GTG CCC AGT CAT AGC CGA ATA GCC TCT CCA CCC AAG. PCR reactions were performed with 100 ng of mouse genomic DNA, to give a total of 25 μl, including the PCR buffer (10 mM Tris-HCl (pH-9.0), 50 mM KCl, 2.5 mM $MgCl_2$ and 0.1% Triton X-100) containing 0.5 U of *Taq* DNA polymerase and 0.2 mM deoxynucleoside triphosphates. The reaction was carried out with an initial 1 min at 96°C followed by 40 cycles of denaturation at 96°C for 45 s, annealing at 70°C for 45 s, extension at 72°C for 6 min, ending with 72°C for 10 min and a hold at 4°C The PCR fragments are approximately 300 bp for the WT allele and between 500–600 bp for the null alleles.

Western blot analysis of Sparc *in WT and null spleens*

Protein was isolated using a single detergent lysis buffer as reported.[14] Protein concentration was determined using the BCA protein assay kit (Pierce Chemical, Rockford, IL, USA). Samples (30 μg) were evaluated by Western blotting as previously reported,[14] except using anti-mouse *Sparc* antibody (catalog no. AF942, R&D Systems, Minneapolis, MN, USA). Actin detection (1:500, no. sc-1616 (Santa Cruz Biotechnology, Santa Cruz, CA, USA)) was used as a loading control.

Wet weights and dry weights

All animal experiments were conducted under approved IACUC protocols. Blood was collected for the blood

smear analyses (see later), and then immune and non-immune organs (spleen, thymus, kidneys, liver and heart) were removed. The organs were weighed immediately for wet weight, dried overnight and weighed the next morning for dry weight ($n=17$ null; $n=11$ WT; of these $n=14$ male subjects; $n=14$ female subjects).

Morphological assessment of organs
Mice were perfused with saline followed by 10% formalin. The organs were removed, weighed and placed in vials containing 10% neutral buffered formalin. Formalin-fixed tissues were embedded in paraffin, sectioned (5 μm) and H&E stained for histomorphological assessment by a hematopathologist (RCH) and a neuropathologist (JAG) ($n=8$/group). For frozen tissues, mice were euthanized and the spleens were immediately snap frozen by liquid nitrogen.

Immunohistochemistry
All reagents are from Biocare Medical (Concord, CA, USA) unless otherwise noted and all incubations were at room temperature. Formalin-fixed, paraffin embedded 4-μm sections were dried in a 60°C oven for 1 h, deparaffinized to water and treated with a peroxidase block. Heat-induced antigen retrieval was used for both *Sparc* and Ki-67, using Diva in a pressure cooker or citrate buffer (pH 6.0) on a hotplate, respectively. Slides for CD31 were treated with trypsin for 15 min at room temperature. Immunohistochemistry was performed on the Biocare Nemesis 7200 autostainer. Sections were blocked in Sniper for 7 min and then incubated in 1:200 anti-*Sparc* (R&D Systems, no. AF942) for 45 min, or 1:250 Ki-67 (Dako (Carpinteria, CA, USA) no. M7249) for 40 min or CD31 (Biocare CM 303) for 3 h. Detection for *Sparc* was biotinylated anti-goat (Vector Laboratories (Burlingame, CA, USA) no. BA5000), for Ki-67 was biotinylated anti-rat (Vector Labs no. BA4001) followed by 4+ horseradish peroxidase (HRP) and Betazoid diaminobenzidine (DAB). CD31 detection was Rat on Mouse HRP Polymer per the manufacturer's instructions, followed by Betazoid DAB. All sections were briefly counterstained in CAT hematoxylin ($n=4$/genotype).

Snap frozen spleens were cut at 8-μm and the sections were picked up onto charged slides. They were air dried at room temperature overnight. They were fixed with two cycles of acetone for 10 min and air drying for 20 min. All reagents used, except for the antibodies, were purchased from Biocare Medical (Concord, CA, USA) and all washes were with Tris-buffered saline with triton (TBST). The procedure was carried out manually. Sections were incubated with Sniper block for 10 min, followed by incubation with rat anti-mouse MOMA-1 (1:80 in green diluent, Serotec (Raleigh, NC, USA) MCA947) at room temperature for 1 h. After a TBST rinse, the sections were incubated with anti-rat polymer-HRP 2 component detection per the manufacturer's instructions, and then incubated with Betazoid DAB for 4 min. Sections were then placed in denature solution (1:1 dilution) for 1.5 min, rinsed in TBST, and then exposed to DAB Sparkle enhancer for 1 min. After a TBST rinse, the sections were incubated with rat anti-mouse IgM (Southern Biotech (Birmingham, AL, USA) 1140-01) diluted 1:3000 in a 1:1 mix of green diluent and Sniper block for 50 min. After a TBST rinse, the sections were then incubated with anti-rat polymer-Alk Phos 2 component detection per instructions. The sections were given a TBST rinse, followed by Ferangi Blue chromogen for 10 min. Sections were mounted after counterstaining in Nuclear Fast Red for 15 s ($n=3$/group).

Quantitation of proliferative germinal center B cells
For each spleen, Ki-67-positive cells were manually counted in the germinal centers or red pulp regions over the entire section. The highest 10 counts for each compartment were averaged for each section. The average number of Ki-67-positive cells was compared between WT and null spleens ($n=4$/group).

Quantitation of marginal zone cell layers
For each spleen, five representative follicles were imaged. For each follicle, the marginal zone cell layers surrounding the follicle were counted manually. For each follicle, the cell layers in 2–3 separate regions were averaged. The counts per follicle for the five representative follicles were then averaged for each spleen. The average number of marginal zone cell layers was compared between WT and null spleens ($n=4$/group).

Quantification of white pulp
For each spleen, $\times 40$ magnification images were captured. The total area and the areas of the white pulp were measured using Pro-Cite image analysis software. For each spleen, the area for the white pulp was calculated as a percentage of the total area. The percentages for each spleen/genotype were then averaged. The average percent area for white pulp was compared between WT and null spleens ($n=4$/group).

Imaging
Immunohistological images were taken at room temperature using a Nikon Eclipse E800M microscope with $\times 10$, $\times 20$ and $\times 40$ objectives connected to a Nikon DXM1200C digital camera, and digitized using ACT-1C software on Dell Optiplex GX620 computers. Tiff images were imported into Adobe Photoshop for composite production. Insets are magnifications performed using Photoshop.

Blood smears and blood smear cell counts
Ethylenediaminetetraacetic acid anticoagulated peripheral blood (40 μl) was used to prepare smears following the wedge method. Four smears were prepared for each sample using precleaned super frost microscope slides (Fisher Scientific, Pittsburg, PA, USA). Smears were fixed by air drying before staining with TruColor Wright Stain (Beckman Coulter, Miami, FL, USA) following the manufacturer's instructions. A manual differential count of 100 WBCs was performed using the thin area of each slide. WBCs were classified as neutrophils, lymphocytes or monocytes based on morphological differences. The counts obtained for each set of four slides were analyzed using Excel software. The smears were reviewed by a hematopathologist (RCH) for morphological assessment ($n=17$ null; $n=11$ WT). The same animals were used for the wet and dry weight assessments.

Hematologic analyses
Mice were anesthetized for orbital blood collection. Blood was collected directly into 3.8% sodium citrate

tubes (1:9 ratio of citrate to blood) and inverted immediately. Basophil, eosinophil, neutrophil, hematocrit, hemoglobin, lymphocyte, monocyte, platelet, WBC and red blood cell numbers were counted from whole blood using ABX Pentra 60C+ (Horiba ABX-USA, Irvine, CA, USA). Data from three experiments were combined for a total $n=26$ null and a total $n=30$ WT mice (experiment no. 1 $n=10$ null, $n=12$ WT; experiment no. 2 $n=6$ null, $n=8$ WT; experiment no. 3 $n=10$ null, $n=10$ WT).

Analysis of immune components

Peripheral blood, spleens and bone marrow were collected for isolation of lymphocytes. Cells were isolated by Ficoll–Hypaque (Amersham Biosciences, Piscataway, NJ, USA) centrifugation separation as described previously.[38] Following this, the primary antibodies CD3 (Santa Cruz Biotechnology), CD19 (GeneTex Inc., San Antonia, TX, USA), CD4, CD8 (Serotec), CD45RA (BDPharmingen, San Jose, CA, USA), CD44, CD11c, CD14 and CD69 (eBioscience, San Diego CA, USA) were used singly or in combination as follows: CD3, CD4, CD8, CD44, CD3/CD44, CD19, CD19/CD44, CD11C, CD3+/CD8−/CD11C+, CD45RA, CD45RAHI, CD45RAMID, CD3/CD45RA, CD3+/CD45RAHI, CD3+/CD45RAMID, CD19/CD45RA, CD19+/CD45RAHI, CD19+/CD45RAMID, CD3+/CD44HI, CD3+/CD44MID, CD19+/CD44HI, CD19+/CD44MID. Secondary antibodies used were fluorescein isothiocyanate (FITC) anti-rabbit, AlexaFLuor 647 anti-rat (Invitrogen, Carlsbad, CA, USA), FITC anti-rat or PE anti-rat (Vector Laboratories, Burlingame, CA, USA). Controls were stained with secondary combinations only. A total of 10^4 events, gated for lymphocytes using forward and side scatter profiles were collected using a FacsCaliber (BDPharmingen) flow cytometer and analyzed using CellQuest software ($n=10$ for each genotype; $n=5$ for each gender with a genotype).

Footpad swelling response

Sparc WT and null mice were injected with 2.5 μg LPS (Sigma Co, St Louis, MO, USA) or sterile PBS alone. Footpad dimension was measured before and every 24 h for 4 days. Degree of swelling is given in mm as the difference between swelling responses at time measured versus original measurement before injection ($n=5$/genotype/group).

Statistical analyses

Two sample *t*-tests were used to compare differences between *Sparc*-null and WT mice for animal weights, organ wet and dry weights, spleen-to-whole body weight ratios, blood smear analyses, Ki-67 proliferation, white pulp and marginal zone cell layer measurements, and cell marker (blood, bone marrow and spleen) measurements. Generalized estimating equation methods were used to compare the two groups for hematologic assessment. These equations take into account that three separate experiments were conducted for hematologic outcomes. For the footpad analyses, Student's *t*-tests and Wilcoxon tests were carried out to compare the groups within genotypes and genotypes within groups. Comparisons were made for all animals, and in some cases for male subjects and female subjects separately. The testing level was set at 0.05 for all comparisons.

Acknowledgements

We are grateful to Dr Chin Howe for the *Sparc*-null mice. We thank Dr Hynda K Kleinman for her thoughtful discussion. This work was supported in part by the NIH/NCI Grant CA086997 (SAR). We are grateful for the continued support of the Barbara Jane Levy and the Gayle Halperin Kahn Funds.

References

1 Gilmour DT, Lyon GJ, Carlton MB, Sanes JR, Cunningham JM, Anderson JR *et al.* Mice deficient for the secreted glycoprotein *SPARC*/osteonectin/BM40 develop normally but show severe age-onset cataract formation and disruption of the lens. *EMBO J* 1998; **17**: 1860–1870.
2 Norose K, Clark JI, Syed NA, Basu A, Heber-Katz E, Sage EH *et al. SPARC* deficiency leads to early-onset cataractogenesis. *Invest Ophthalmol Vis Sci* 1998; **39**: 2674–2680.
3 Delany AM, Kalajzic I, Bradshaw AD, Sage EH, Canalis E. Osteonectin-null mutation compromises osteoblast formation, maturation, and survival. *Endocrinology* 2003; **144**: 2588–2596.
4 Bradshaw AD, Graves DC, Motamed K, Sage EH. *SPARC*-null mice exhibit increased adiposity without significant differences in overall body weight. *Proc Natl Acad Sci USA* 2003; **100**: 6045–6050.
5 Bradshaw AD, Reed MJ, Sage EH. *SPARC*-null mice exhibit accelerated cutaneous wound closure. *J Histochem Cytochem* 2002; **50**: 1–10. Erratum in: *J Histochem Cytochem* 2002; **50**: 875.
6 Puolakkainen PA, Brekken RA, Muneer S, Sage EH. Enhanced growth of pancreatic tumors in *SPARC*-null mice is associated with decreased deposition of extracellular matrix and reduced tumor cell apoptosis. *Mol Cancer Res* 2004; **2**: 215–224.
7 Bos TJ, Cohn SL, Kleinman HK, Murphy-Ulrich JE, Podhajcer OL, Rempel SA *et al.* International Hermelin brain tumor symposium on matricellular proteins in normal and cancer cell-matrix interactions. *Matrix Biol* 2004; **23**: 63–69.
8 Mok SC, Chan WY, Wong KK, Cheung KK, Lav CC, Ng SW *et al. SPARC*, an extracellular matrix protein with tumor-suppressing activity in human ovarian epithelial cells. *Oncogene* 1996; **12**: 1895–1901.
9 Said N, Motamed K. Absence of host-secreted protein acidic and rich in cysteine (*SPARC*) augments peritoneal ovarian carcinomatosis. *Am J Pathol* 2005; **167**: 1739–1752.
10 Yiu GK, Chan WY, Ng SW, Chan PS, Cheung KK, Berkowitz RS *et al. SPARC* (secreted protein acidic and rich in cysteine) induces apoptosis in ovarian cancer cells. *Am J Pathol* 2001; **159**: 609–622.
11 Chlenski A, Liu S, Crawford SE, Volpert OV, DeVries GH, Evangelista A *et al. SPARC* is a key Schwannian-derived inhibitor controlling neuroblastoma tumor angiogenesis. *Cancer Res* 2002; **62**: 7357–7363.
12 Chlenski A, Liu S, Baker LJ, Yang Q, Tian Y, Salwen HR *et al.* Neuroblastoma angiogenesis is inhibited with a folded synthetic molecule corresponding to the epidermal growth factor-like module of the follistatin domain of *SPARC*. *Cancer Res* 2004; **64**: 7420–7425.
13 Ledda F, Bravo AI, Adris S, Bover L, Mordoh J, Podhajcer OL. The expression of the secreted protein acidic and rich in cysteine (*SPARC*) is associated with the neoplastic progression of human melanoma. *J Invest Dermatol* 1997a; **108**: 210–214.
14 Rempel SA, Golembieski WA, Ge S, Lemke N, Elisevich K, Mikkelsen T *et al. SPARC*: a signal of astrocytic neoplastic transformation and reactive response in human primary and xenograft gliomas. *J Neuropathol Exp Neurol* 1998; **57**: 1112–1121.
15 Ledda MF, Adris S, Bravo AI, Kairiyama C, Bover L, Chernajovsky Y *et al.* Suppression of *SPARC* expression by

antisense RNA abrogates the tumorigenicity of human melanoma cells. *Nat Med* 1997a; **3**: 171–176.
16 Golembieski WA, Ge S, Nelson K, Mikkelsen T, Rempel SA. Increased *SPARC* expression promotes U87 glioblastoma invasion *in vitro*. *Int J Dev Neurosci* 1999; **17**: 463–472.
17 Schultz C, Lemke N, Ge S, Golembieski WA, Rempel SA. Secreted protein acidic and rich in cysteine promotes glioma invasion and delays tumor growth *in vivo*. *Cancer Res* 2002; **62**: 6270–6277.
18 Sangaletti S, Stoppacciaro A, Guiducci C, Torrisi MR, Columbo MP. Leukocyte, rather than tumor-produced *SPARC*, determines stroma and collagen type IV deposition in mammary carcinoma. *J Exp Med* 2003; **98**: 1475–1485.
19 Brekken RA, Puolakkainen P, Graves DC, Workman G, Lubkin SR, Sage EH. Enhanced growth of tumors in *SPARC* null mice is associated with changes in the ECM. *J Clin Invest* 2003; **111**: 487–495.
20 Puolakkainen PA, Brekken RA, Muneer S, Sage EH. Enhanced growth of pancreatic tumors in *SPARC*-null mice is associated with decreased deposition of extracellular matrix and reduced tumor cell apoptosis. *Mol Cancer Res* 2004; **2**: 215–224.
21 Alvarez MJ, Prada F, Salvatierra E, Bravo AI, Lutzky VP, Carbone C *et al*. Secreted protein acidic and rich in cysteine produced by human melanoma cells modulates polymorphonuclear leukocyte recruitment and antitumor cytotoxic capacity. *Cancer Res* 2005; **65**: 5123–5132.
22 Savani RC, Zhou Z, Arguiri E, Wang S, Vu D, Howe CC *et al*. Bleomycin-induced pulmonary injury in mice deficient in *SPARC*. *Am J Physiol Lung Cell Mol Physiol* 2000; **279**: L743–L750.
23 Sangaletti S, Gioiosa L, Guiducci C, Rotta G, Rescigno M, Stoppacciaro A *et al*. Accelerated dendritic-cell migration and T-cell priming in *SPARC*-deficient mice. *J Cell Science* 2005; **118**: 3685–3694.
24 Aycock RL, Bradshaw AC, Sage EH, Starcher B. Development of UV-induced squamous cell carcinomas is suppressed in the absence of *SPARC*. *J Invest Dermatol* 2004; **123**: 592–599.
25 Sage EH, Vernon RB, Decker J, Funk S, Iruela-Arispe ML. Distribution of the calcium-binding protein *SPARC* in tissues of embryonic and adult mice. *J Histochem Cytochem* 1989; **37**: 819–829.
26 Shen Y, Iqbal J, Xiao L, Lynch RC, Rosenwald A, Staudt LM *et al*. Distinct gene expression profiles in different B-cell compartments in human peripheral lymphoid organs. *BMC Immunol* 2004; **5**: 20.
27 Kzhyshkowska J, Gratchev A, Goerdt S. Stabilin-1, a homeostatic scavenger receptor with multiple functions. *J Cell Mol Med* 2006; **10**: 635–649.
28 Kzhyshkowska J, Workman G, Cardo-Vila M, Arap W, Pasqualini R, Gratchev A *et al*. Novel function of alternatively activated macrophages: stabilin-1-mediated clearance of *SPARC*. *J Immunol* 2006; **176**: 5825–5832.
29 Kelly KA, Allport JR, Yu AM, Sinh S, Sage EH, Gerszten RE *et al*. *SPARC* is a VCAM-1 counter-ligand that mediates leukocyte transmigration. *J Leukoc Biol* December 18 (E-pub ahead of print).
30 Pillai S, Cariappa A, Moran ST. Marginal zone B cells. *Ann Rev Immunol* 2005; **23**: 161–196.
31 Lopes-Carvalho T, Kearney JF. Development and selection of marginal zone B cells. *Immunol Rev* 2004; **197**: 192–205.
32 Cariappa A, Tang M, Parng C, Nebelitskiy E, Carroll M, Georgopoulos K *et al*. The follicular versus marginal zone B lymphocyte cell fate decision is regulated by Aiolos, Btk, and CD21. *Immunity* 2001; **14**: 603–615.
33 Guinamard R, Okigaki M, Schlesinger J, Ravetch JV. Absence of marginal zone B cells in Pyk-2-deficient mice defines their role in the humoral response. *Nature Immunol* 2000; **1**: 31–36.
34 Bradshaw AD, Sage EH. *SPARC*, a matricellular protein that functions in cellular differentiation and tissue response to injury. *J Clin Invest* 2001; **107**: 1049–1054.
35 Oritani K, Kincade PW. Identification of stromal cell products that interact with pre-B cells. *J Cell Biol* 1996; **134**: 771–782.
36 Stary M, Pasteiner W, Summer A, Hrdina A, Eger A, Weitzer G *et al*. Parietal endoderm secreted *SPARC* promotes early cardiomyogenesis *in vitro*. *Exp Cell Res* 2005; **310**: 331–343.
37 Ishimoto H, Ginzinger DG, Matsumoto T, Hattori Y, Furuya M, Minegishi K *et al*. Differential zonal expression and adrenocorticotropin regulation of secreted protein acidic and rich in cysteine (*SPARC*), a matricellular protein, in the midgestation human fetal adrenal gland: implications for adrenal development. *J Clin Endocrin Metab* 2003; **91**: 3208–3214.
38 Chi DS, Harris NS. A simple method for the isolation of murine peripheral blood lymphocytes. *J Immunol Methods* 1978; **19**: 169–172.